

Monolayer graphene film/silicon nanowire array Schottky junction solar cells

Chao Xie,^{1,2} Peng Lv,¹ Biao Nie,¹ Jiansheng Jie,^{1,a)} Xiwei Zhang,¹ Zhi Wang,¹ Peng Jiang,¹ Zhizhong Hu,¹ Linbao Luo,^{1,b)} Zhifeng Zhu,¹ Li Wang,¹ and Chunyan Wu¹

¹*School of Electronic Science and Applied Physics, Hefei University of Technology, Hefei Anhui 230009, People's Republic of China*

²*School of Materials Science and Engineering, Hefei University of Technology, Hefei Anhui 230009, People's Republic of China*

(Received 29 June 2011; accepted 31 August 2011; published online 28 September 2011)

Schottky junction solar cells were constructed by combining the monolayer graphene (MLG) films and the Si nanowire (SiNW) arrays. Pronounced photovoltaic characteristics were investigated for devices with both p-MLG/n-SiNWs and n-MLG/p-SiNWs structures. Due to the balance between light absorption and surface carrier recombination, devices made of SiNW arrays with a medium length showed better performance and could be further improved by enhancing the MLG conductivity via appropriate surface treatment or doping. Eventually, a photoconversion efficiency up to 2.15% is obtained by the means of filling the interspace of SiNW array with graphene suspension. © 2011 American Institute of Physics. [doi:10.1063/1.3643473]

Silicon is the leading material in commercial solar cell modules, accounting for about 90% of the global photovoltaic market. Compared with their thin film counterparts, silicon nanowires (SiNWs) have exhibited unique properties in terms of light absorption and electron transport.^{1,2} By this token, SiNW-based solar cells have lately received increasing interest for their potential in the next-generation solar energy conversion devices.³ Peng *et al.* reported on the photovoltaic application of platinum nanoparticles decorated SiNW arrays synthesized by a HF etching method.⁴ What is more, hybrid solar cells consisting of SiNW arrays and P3HT:PCBM with efficiency of 1.9% were also reported.⁵

The selection of appropriate electrode materials is of vital importance to the device performance. Generally, high photoconversion efficiency necessitates transparent electrodes for solar light transmission and good electrical conduction for carriers transport. This is contradictory for most of the thin film transparent electrodes available, as their thickness is normally proportionate to electrical conduction while inversely proportionate to transparency. The discovery of highly transparent graphene thin film with carrier mobility as high as 200 000 cm²/Vs provides a solution to this challenge. Li *et al.* reported the few-layer graphene (FLG)/Si substrate Schottky junction solar cells with power conversion efficiency of 2.2%.⁶ Fan *et al.* also demonstrated the FLG/SiNW solar cells with efficiency of 2.86%, as a consequence of enhanced light trapping and faster carrier transport.⁷ In spite of these progresses, the utilization of monolayer graphene (MLG), which possess higher transparency leading to more light absorption in photovoltaic devices and inherits most of the striking properties of graphene, as building block for SiNW-based solar cells remains less explored and understood.⁸

In this work, we extensively studied the photovoltaic characteristics of the solar cells composed of MLG films and SiNW arrays, and totally eight types of solar cells with vari-

ous device configurations were investigated. A maximum efficiency of 2.15% was achieved by optimizing the device structures and further filling the interspace of the SiNW array with graphene suspension.

The vertical SiNW arrays were prepared via an Ag-assisted chemical etching method.⁹ Both n- and p-type Si wafers (resistivity: 5–15 Ωcm⁻¹) were used. After etching, the as-obtained SiNW arrays were dipped into a diluted HNO₃ and HF solution to dissolve Ag and SiO₂ on the SiNWs surface, respectively. The MLG films were prepared at 1000 °C by using a mixed gas of CH₄ (40 SCCM) and H₂ (20 SCCM) via chemical vapor deposition (CVD),¹⁰ and 25 μm thick Cu foil was employed as the catalytic substrate. Nitrogen-doped MLG films were synthesized at the same conditions except the introduction of NH₃ as the dopant.¹¹ After growth, the MLG films were spin-coated with 5 wt. %

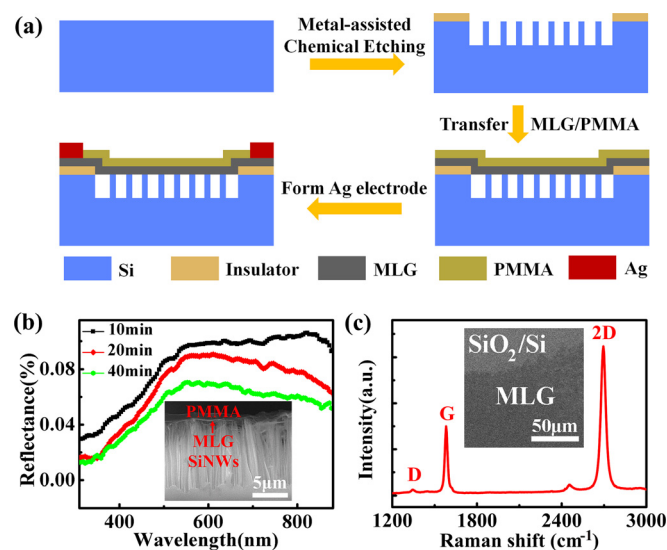


FIG. 1. (Color online) (a) Schematic illustration of the fabrication process for the MLG film/SiNW array Schottky junction solar cell. (b) Reflection spectra of SiNW arrays obtained from 10, 20, and 40 min etching. Inset shows cross-sectional SEM image of SiNW array with PMMA-supported MLG film on it. (c) Raman spectrum of the MLG film. Inset shows the SEM image of the isolated MLG film on SiO₂/Si substrate.

^{a)}Author to whom correspondence should be addressed. Electronic mail: jason.jsjie@gmail.com.

^{b)}Electronic mail: luolb@hfu.edu.cn.

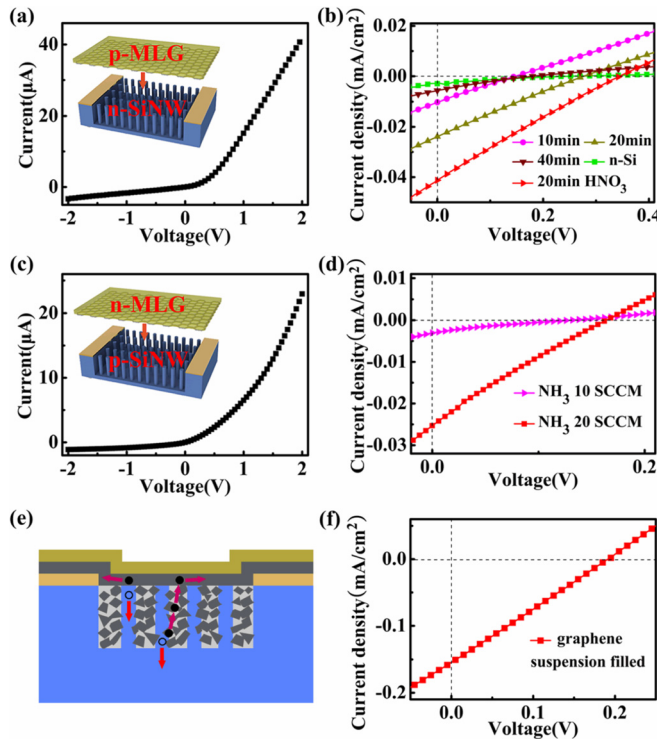


FIG. 2. (Color online) Dark I - V curve of device A4 (a), device B2 (c). Inset in (a), (c), and (e) shows the schematic illustration of p-MLG/n-SiNW Schottky junction, n-MLG/p-SiNW solar cells, and graphene suspension filled solar cell, respectively. J - V curves of p-MLG/n-SiNW solar cells for devices A0, A1, A2, A3, and A4 (b), n-MLG/p-SiNW solar cells for devices B1 and B2 (d), device C1 (f).

polymethylmethacrylate (PMMA) in chlorobenzene, and the underlying Cu foils were removed in Marble's reagent solution ($\text{CuSO}_4\text{:HCl:H}_2\text{O} = 10\text{ g:50 ml:50 ml}$). To construct the solar cells, the PMMA-supported MLG films were directly transferred onto the top of the SiNW arrays. For insulating purpose, sellotape was stuck at the four edges of the mother Si substrates before the preparation of SiNW arrays. Ag paste contacts formed at the corners of the MLG films and the back side of the Si substrates acted as the top and back electrodes, respectively. The step-wise process for the device construction was illustrated in Figure 1(a). The photovoltaic characteristics of the MLG/SiNW solar cells were evaluated by Keithley 4200 SCS under the white light illumination ($350\text{ }\mu\text{Wcm}^{-2}$).

Figure 1(b) depicts the reflection spectra of SiNW arrays synthesized via 10, 20, and 40 min etching, in which, light absorption was observed to increase with length increase.

Further Raman spectrum in Fig. 1(c) is found to be composed of two sharp peaks, i.e., 2D-band peak at $\sim 2695\text{ cm}^{-1}$ and G-band peak at $\sim 1581\text{ cm}^{-1}$. The intensity ratio of I_{2D} : $I_G \approx 2.2$, combined with the weak D-band scattering at $\sim 1343\text{ cm}^{-1}$, confirms the high crystal quality of the monolayer graphene film.¹²

First, different Schottky junction solar cells composed of the MLG, generally known to exhibit weak p-type conductivity,¹² and n-SiNWs were evaluated [Figs. 2(a) and 2(b), and devices A1-A4 in Table I]. By virtue of the formation of Schottky barrier, excellent rectification characteristics are observed [Fig. 2(a)]. Moreover, these devices exhibit pronounced photovoltaic effects upon white light illumination. As shown in Fig. 2(b), the device made of n-Si wafer (A0) shows the worst performance, with a power conversion efficiency (η) of 0.04%. In contrast, substantial increase of η to 0.10% is observed, when silicon wafer was replaced with SiNW array etched for 10 min (A1). The conversion efficiency continues to increase to a maximum value of 0.40% for device made of 20 min etched SiNW array (A2), near ten times of the initial value for Si wafer. Nevertheless, further prolongation of the etching time (40 min, A3) results in the degeneration of the device performance. Interestingly, enhancement of p-type conductivity of the MLG via HNO_3 treatment can considerably increase the η value to 0.95%.¹³

Remarkably, good rectification and photovoltaic effects are observed in the n-MLG/p-SiNW Schottky junctions (B1 and B2) as well [Figs. 2(c) and 2(d)]. It can be found that the device performance increases with the N doping level, which could be attributed to the enhanced n-type conductivity of the MLG film at higher N doping concentration. However, we note that the overall performance of B1 and B2 is still worse than A2 and A4. The lower sheet conductivity of the N-doped graphene compared to pristine graphene might be an important reason.^{11,14}

To understand the work mechanism of the MLG/SiNW Schottky junction solar cells, photoresponse characteristics of both p-MLG/n-SiNW and n-MLG/p-SiNW devices were investigated [Figs. 3(a) and 3(b)]. The observed high sensitivity to the light illumination with a large $I_{\text{on}}/I_{\text{off}}$ ratio $> 10^3$, along with the fast response speed, signifies that the electron-hole pairs could be efficiently generated and separated in the MLG/SiNW solar cells, which helps facilitate the Schottky junctions to harvest solar light more effectively. On the other hand, such photoresponse behavior is highly reversible and reproducible, implying that our devices can also function as high-performance photodetectors that could

TABLE I. Device performances of MLG film/SiNW array Schottky junction solar cells.

Sample		V_{OC} (V)	J_{SC} (μ A/cm ²)	FF	η (%)
A0	n-Si pristine MLG	0.25	3.0	0.19	0.04
A1	10 min n-SiNWs pristine MLG	0.15	10.3	0.24	0.10
A2	20 min n-SiNWs pristine MLG	0.24	22.3	0.26	0.40
A3	40 min n-SiNWs pristine MLG	0.15	5.3	0.24	0.05
A4	20 min n-SiNWs p-MLG (HNO ₃ treated)	0.35	41.2	0.23	0.95
B1	20 min p-SiNWs n-MLG (10SCCM NH ₃)	0.13	2.8	0.19	0.02
B2	20 min p-SiNWs n-MLG (20SCCM NH ₃)	0.16	25.3	0.23	0.27
C1	20 min n-SiNWs pristine MLG (grapheme Suspension filled)	0.19	154.5	0.25	2.15

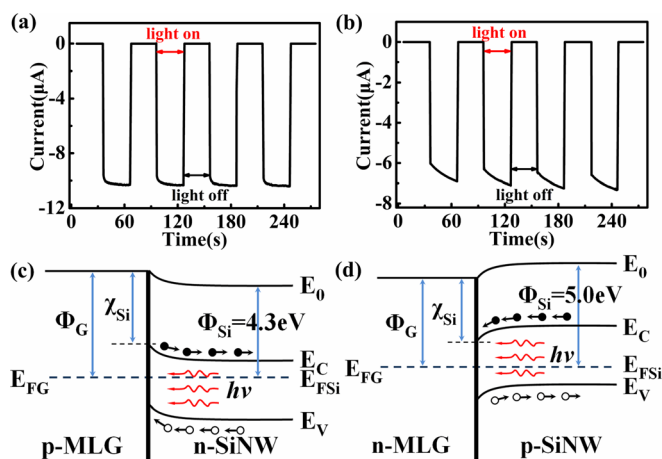


FIG. 3. (Color online) Photoresponse of devices A4 (a) and B2 (b) at zero bias. (c) and (d) are energy diagrams of p-MLG/n-SiNW and n-MLG/p-SiNW Schottky junctions upon light illumination, respectively. Φ_G/Φ_{Si} and E_{FG}/E_{FSi} denote the work functions and Fermi energy levels of graphene/SiNW. χ_{Si} is the electron affinity of silicon. E_C and E_V are the conduction band and valence band of silicon, respectively.

operate at zero bias voltage. Besides the fast rise edge, a slow rise edge is observed for device B2. Doping induced defects in the graphene is likely responsible for this result since the trap centers have to be filled upon light illumination before the system can finally reach equilibrium.¹⁴

Figs. 3(c) and 3(d) show the energy band diagrams of p-MLG/n-SiNW and n-MLG/p-SiNW, respectively. As a result of the formation of Schottky barrier at the MLG/SiNW interface, partial carriers in SiNWs tend to move to the graphene side and consequently the energy levels near the SiNW surface will bend upward (for n-SiNW) or downward (for p-SiNW), causing the formation of space-charge region and built-in electric field near the MLG/SiNW interface. Upon light illumination, the photogenerated electron-hole pairs will be separated within the built-in field region, and the resulted free electrons and holes will move towards opposite directions, which results in the generation of the photocurrent. This model suggests that the MLG films serve not only as transparent electrodes but also as important active layers in the devices.

It is noted that though longer SiNW array is beneficial to the light trapping and absorption, which is essential for high-performance solar cells, it does not follow that increase in length will necessarily lead to higher photoconversion efficiency, considering the severe surface carrier recombination induced by the large amount of surface defects.¹ This can explain well why the devices made of SiNW array with medium length (A2, A4) display the highest efficiency. Furthermore, the device performance is also associated with the electrical properties of the MLG films. As discussed before, HNO_3 treatment or N-doping on the MLG films can increase the Schottky barrier by improving the graphene's conductivity, which will further cause the broadening of the space-charge region in SiNW and the strengthening of the built-in field. As a result, the photogenerated carriers could be separated and transport more efficiently, giving rise to the higher photoconversion efficiency.

Undeniably, the photoconversion efficiency of the photovoltaic devices is relatively low. We attribute this to the small Schottky junction area as well as the long distance the photogenerated carriers have to travel, which are predetermined by the device configurations. In this connection, graphene suspension that compose of small graphene sheets ($0.5\text{--}5\text{ }\mu\text{m}$) was placed at the interspace of the SiNW array before the transfer of MLG film [Fig. 2(e)], in order to facilitate carrier separation and transport by enlarging the contact area. Indeed, C1 exhibits a much improved short-circuit current density (J_{sc}) of $154.5\text{ }\mu\text{A cm}^{-2}$ [Fig. 2(f)], nearly seven times of that of A2. Accordingly, a large η value of 2.15% is achieved for this device. It should be mentioned that the fill factors (FF) of our MLG/SiNW devices (0.19-0.26) are still much lower than the commercial Si solar cells (~ 0.80). The load resistance comes from the MLG film and the electrode contact might be responsible for the low value.

In conclusion, Schottky junction solar cells composed of MLG films and SiNW arrays were fabricated. Devices with both p-MLG/n-SiNW and n-MLG/p-SiNW structures were investigated and they show pronounced photovoltaic effects under the light illumination. Optimization to the devices leads to a photoconversion efficiency of 2.15%. The simple and low-cost fabrication process of the MLG/SiNW Schottky junctions makes it a promising candidate for future high-performance solar cell applications.

This work was supported by the National Natural Science Foundation of China (Nos. 60806028, 51172151, 20901021, 61106010, 21101051), the Program for New Century Excellent Talents in University of the Chinese Ministry of Education (NCET-08-0764), the Major Research Plan of the National Natural Science Foundation of China (No. 91027021), and National Basic Research Program of China (No. 2012CB932400).

¹E. Garnett and P. D. Yang, *Nano Lett.* **10**, 1082 (2010).

²J. S. Jie, W. J. Zhang, K. Q. Peng, G. D. Yuan, C. S. Lee, and S. T. Lee, *Adv. Funct. Mater.* **18**, 3251 (2008).

³V. Sivakov, G. Andr, A. Gawlik, A. Berger, J. Plentz, F. Falk, and S. H. Christiansen, *Nano Lett.* **9**, 1549 (2009).

⁴K. Q. Peng, X. Wang, X. L. Wu, and S. T. Lee, *Nano Lett.* **9**, 3704 (2009).

⁵J. S. Huang, C. Y. Hsiao, S. J. Syu, J. J. Chao, and C. F. Lin, *Sol. Energy Mater. Sol. Cells* **93**, 621 (2009).

⁶X. M. Li, H. W. Zhu, K. L. Wang, A. Y. Cao, J. Q. Wei, C. Y. Li, Y. Jia, Z. Li, X. Li, and D. H. Wu, *Adv. Mater.* **22**, 2743 (2010).

⁷G. F. Fan, H. W. Zhu, K. L. Wang, J. Q. Wei, X. M. Li, Q. K. Shu, N. Guo, and D. H. Wu, *Appl. Mater. Interface* **3**, 721 (2011).

⁸R. R. Nair, P. Blake, A. N. Grigorenko, K. S. Novoselov, T. J. Booth, T. Stauber, N. M. T. Peres, and A. K. Geim, *Science* **320**, 1308 (2008).

⁹M. L. Zhang, K. Q. Peng, X. Fan, J. S. Jie, R. Q. Zhang, S. T. Lee, and N. B. Wong, *J. Phys. Chem. C* **112**, 4444 (2008).

¹⁰X. S. Li, W. W. Cai, J. H. An, S. Y. Kim, J. H. Nah, D. X. Yang, R. Piner, A. Velamakanni, I. W. Jung, E. Tutuc, S. K. Banerjee, L. Colombo, and R. S. Ruoff, *Science* **324**, 1312 (2009).

¹¹D. C. Wei, Y. Q. Liu, Y. Wang, H. L. Zhang, L. P. Huang, and G. Yu, *Nano Lett.* **9**, 1752 (2009).

¹²A. Reina, X. T. Jia, J. Ho, D. Nezich, H. Son, V. Bulovic, M. S. Dresselhaus, and J. Kong, *Nano Lett.* **9**, 30 (2009).

¹³S. K. Bae, H. K. Kim, Y. B. Lee, X. F. Xu, J. S. Park, Y. Zheng, J. Balakrishnan, T. Lei, H. R. Kim, Y. I. Song, Y. J. Kim, K. S. Kim, B. Ozyilmaz, J. H. Ahn, B. H. Hong, and S. Iijima, *Nat. Nanotechnol.* **10**, 1038 (2010).

¹⁴H. T. Liu, Y. Q. Liu, and D. B. Zhua, *J. Mater. Chem.* **21**, 3335 (2011).